Polarization of thick polyvinylidene fluoride/trifluoroethylene copolymer films

H. L. W. Chan,[a] Z. Zhao, K. W. Kwok, and C. L. Choy
Department of Applied Physics and Materials Research Center, The Hong Kong Polytechnic University, Hung Hom, Kowloon, Hong Kong

C. Alquié, C. Boué, and J. Lewiner
Laboratoire d'Electricité Générale, Ecole Supérieure de Physique et de Chimie Industrielles, Paris, France

(Received 31 July 1995; accepted for publication 12 June 1996)

Thick (800 μm) polyvinylidene fluoride/trifluoroethylene (P(VDF-TrFE)) copolymer films for transducer applications are poled under applied voltage at elevated temperatures. By using different heat treatments, poling temperatures, and poling time, we are able to prepare a uniformly poled film with a single resonance peak at 1.3 MHz, or a nonuniformly poled film with two resonances (1.3 and 2.6 MHz), or a film with bimorph structure with a single resonance at 2.6 MHz. The nonuniform polarization which arises from charge injection from the cathode is checked by the pressure wave propagation method. The polarization mechanisms in these thick films are expected to be similar to those previously reported for thin films. The results obtained in this work may lead to practical applications because they suggest a means for controlling transducer frequency by poling. © *1996 American Institute of Physics.* [S0021-8979(96)04818-9]

I. INTRODUCTION

Polyvinylidene fluoride (PVDF) and its copolymers with trifluoroethylene (TrFE) are important piezoelectric materials for transducer applications. Compared to piezoelectric ceramics, PVDF and its copolymers have acoustic impedances closer to that of water and human tissues and have higher voltage constants. The advantage of using P(VDF-TrFE) copolymer is that, for TrFE content above 20%, it crystallizes from the melt or from solution in a polar phase (the β phase); hence it is possible to fabricate transducers of various shapes (e.g., thick slabs or cylinders) and pole the copolymer without prior stretching.[1]

1–3 and 0–3 composites of P(VDF-TrFE) copolymers and piezoelectric ceramics have also attracted considerable interest.[2,3] In a piezoelectric ceramic/piezoelectric copolymer 1–3 composite project some of us are currently working on,[4] fired PZT rods are inserted into a prepoled thick copolymer matrix to form a 1–3 composite and the ceramic rods are then poled at a much lower electric field. Hence it is important to develop a method to pole thick copolymer films properly. Thermal poling at temperatures above 100 °C has been chosen since some of us, also working on a 0–3 PZT/copolymer composite project, have found that 0–3 composites can only be poled at high temperatures.[5] Consequently, information on the high temperature poling characteristics of the copolymer obtained in the present study will help us to optimize the 0–3 composite poling conditions.

In the literature, there are a large number of poling studies on thin (less than 300 μm) PVDF or PVDF-TrFE copolymer films.[6–12] Although studies on the poling of thick copolymer films are rare, the principles governing the polarization mechanisms in thin and thick films are expected to be similar. Various methods have been developed to measure the polarization distribution within a polymer film. The most widely used thermal methods include the thermal pulse method,[13,14] the laser intensity modulation method (LIMM),[15,16] and the thermal step method.[17] The acoustic methods include the pressure wave propagation (PWP) method[18,19] [also known as the laser induced pressure pulse (LIPP) method[20]], the piezoelectrically generated pressure step method[21] and the pulsed electroacoustic method.[22]

It has been shown previously that non-uniform poling of thin P(VDF-TrFE) film can occur, with the polarization starting at the anode, and the mechanism has been discussed in detail.[8,10,11,23–25] In this paper we study the poling of thick copolymer films at elevated temperature. The resonance frequencies of these films have been measured. Similar to the behavior of thin films, the observed effects can also be attributed to nonuniform poling. This was checked by measuring the polarization distribution in the poled films using the PWP method.

II. POLING OF THICK COPOLYMER FILMS

The starting materials are 0.8 mm thick extruded unpoled vinylidene fluoride-trifluoroethylene (80/20) copolymer sheets supplied by Atochem North America Inc. The value of the thickness electromechanical coupling factor k_t is used as a figure of merit to indicate whether the copolymer is adequately poled. A copolymer having this VDF content, when poled, was reported to have the highest k_t value amongst copolymers of different composition.[26]

A. Effect of heat treatment on unpoled samples

Samples are either annealed at 120 °C for 2 h and then cooled to room temperature in the oven after the oven was switched off, or melted and hot pressed at 180 °C for 5 min and then cooled to room temperature in the press after it was

[a]Elecronic mail: polyu@hkpucc.polyu.edu.hk

 0021-8979/96/80(7)/3982/10/$10.00

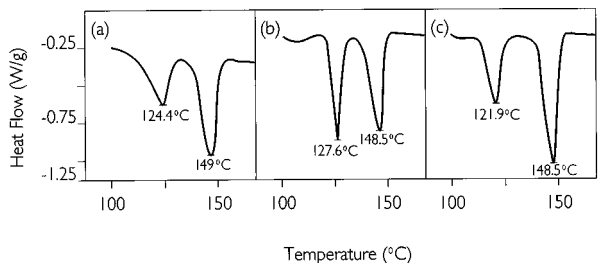

FIG. 1. DSC heating endotherms of unpoled P(VDF-TrFE) (80/20) samples (a) As-received. (b) annealed at 120 °C for 2 h. (c) melted and hot pressed at 180 °C for 5 min.

switched off. The endotherms for unpoled samples with different heat treatments obtained at a heating rate of 10 °C/min using a DuPont 2000 thermal analyzer are given in Fig. 1. The Curie transition temperature for the first heating ($\uparrow T_c$) of the as-received sample is 124.4 °C, which is close to but lower than the reported $\uparrow T_c$ value for this composition,[27] indicating that the TrFE content may be slightly higher than 20%. Because of thermal hysteresis,[28] the Curie temperature obtained for cooling ($\downarrow T_c$) of the original sample is 73 °C. Annealing gives rise to a narrowing of the transition peak and a shift to higher temperature. The crystalline melting temperature T_m remains almost unchanged upon different heat treatments.[26] The melted and hot-pressed sample has a lower $\uparrow T_c$ compared to the as-received sample. This may be due to the fact that the as-received extruded sheets have some chain orientation and melting has wiped out the orientation history of the sample.

X-ray diffraction (XRD) studies using a Philips x-ray diffractometer show that the XRD peaks of the annealed sample are essentially identical to those of the original sample, but there is a slight increase (about 0.5 deg) in the diffraction angle of the major peak (at $2\theta=20$ deg, which is the $(200)\beta+(110)\beta$ peak).[29] The as-received copolymer (with 80% VDF) has a diffractogram [Fig. 2(a)] similar to that reported for this composition.[29] After hot-pressing [Fig. 2(b)], the intensity of the $(200)\beta+(110)\beta$ peak decreases while the intensities of the $(001)\beta$ (at $2\theta=35.06$ deg) and the $(201)\beta$ (at $2\theta=41$ deg) increase. Further annealing of the

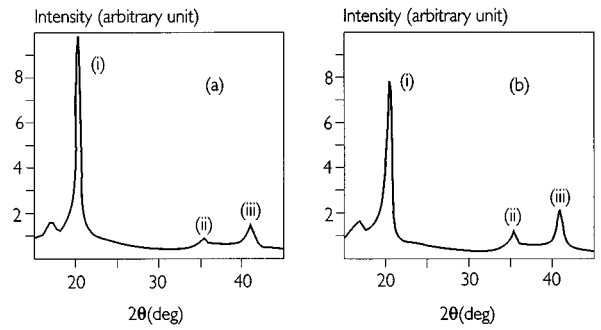

FIG. 2. X-ray diffractograms of the unpoled copolymer samples. (a) As-received (b) melted and hot pressed, (i) $(200)\beta+(110)\beta$, (ii)$(001)\beta$, (iii)$(201)\beta$.

hot-pressed sample at 120 °C for another 2 h does not change its diffractogram.

B. Thermal poling procedures and resonance characteristics of sample after poling

Thermal poling is carried out in a temperature controlled oil bath. A two-side metalized (with silver paint) sample is exposed to a high poling field at an elevated temperature for a period of 1–4 h. The sample is then cooled down to room temperature with the field applied to stabilize the dipole alignment. Several types of film samples are studied. Samples are first annealed at 120 °C for 2 h and then (i) poled at 105 °C for 2 h, (ii) poled at 105 °C for 4 h, (iii) poled using a two-step poling method in which the sample is poled at 105 °C for 2 h, and then cooled down to room temperature with the electric field kept on; then the sample is repoled at 105 °C for another 2 h. Samples are also melted and hot-pressed at 180 °C for 5 min and then (iv) poled at 115 °C for 1 h, (v) poled at 115 °C using the two-step poling method, with 1 h poling time for each poling step.

The electric field applied to each sample is about 30 MV/m. This is very close to its breakdown electric field and is higher than the reported high-temperature coercive field for the copolymer.[30] The annealed and the as-received film cannot withstand such a high electric field when heated up to higher than 105 °C, while the melted and hot-pressed film can be heated to higher temperature and can withstand a higher poling field without breakdown. This shows that the melt and hot-pressed process can improve the dielectric strength of the copolymer films, as reported previously.[27] The poling field is 26 MV/m for the annealed film at 105 °C and 30 MV/m for the hot-pressed film at 115 °C.

After poling, the DSC thermograms of samples (i) to (v) show the following characteristics: for the annealed samples, poling shifted $\uparrow T_c$ to higher temperature, indicating the formation of a more ordered phase. The effect of poling is more pronounced in the hot-pressed samples. The transition peak not only shifted to higher temperature but also became sharper. The densities of the samples are listed in Table I. Both types of heat treatments caused an increase in density, indicating an increase in the amount and quality of the polar β-phase crystallites. During poling, the samples tended to swell and this accounted for the decrease in density. Among the five poled samples, sample (v) has the highest density.

Typical impedance vs frequency plots for samples (i) to (v) are shown in Fig. 3(a) to 3(e), and the values of k_t and d_{33} are given in Table I. The values of k_t were evaluated using the method of Sherrit *et al.*[31] which takes into account the high loss in the copolymer. The d_{33} values were measured using a Pennebaker model 8000 piezo d_{33} tester from American Piezo-Ceramics, Inc., Samples (i), (ii), and (iv) have two resonance peaks, a major peak at about 1.3 MHz and a secondary peak at 2.6 MHz. Judging from the frequencies, the secondary peak is the second harmonic of the first one. However, for thickness mode resonance, the boundary condition excludes the presence of even number harmonics and the second harmonic should not appear. Poling the sample for longer time increases the height of the first peak and decrease the secondary peak. Two step poling com-

TABLE I. Properties of copolymer samples.

Sample	k_t	d_{33} (pCN^{-1})	Density (kg m^{-3})	$\uparrow T_c$(°C)	T_m(°C)	Thickness (mm)	Sound velocity (ms^{-1})
As-received			1864	124.4	149.0	0.81	2246
Annealed			1872	127.6	148.5	0.83	2258
Hot pressed			1884	121.9	148.5	0.69	2304
(i)	0.20	30.5	1846	132.9	150.3	0.79	2285
(ii)	0.25	32.1	1865	130.8	149.6	0.79	2302
(iii)	0.27	36.2	1861	132	148.9	0.79	2289
(iv)	0.21	28.5	1854	127.2	149.6	0.67	2268
(v)	0.29	35.3	1878	128	149.6	0.67	2308
Bimorph	0.25	11.5	1850	125.5	148.9	0.78	2248

pletely eliminates the secondary peak [see Figs. 3(c) and 3(e)]. The appearance of the second harmonic may be ascribed to the nonuniform poling of the thick copolymer films. In order to check this hypothesis, a measurement of the polarization distribution of the poled films was made using the PWP method described in the next section.

III. THE PRESSURE WAVE PROPAGATION (PWP) METHOD

A. Experiments

The experimental setup for the PWP method is shown in Fig. 4. The results presented in this section were obtained

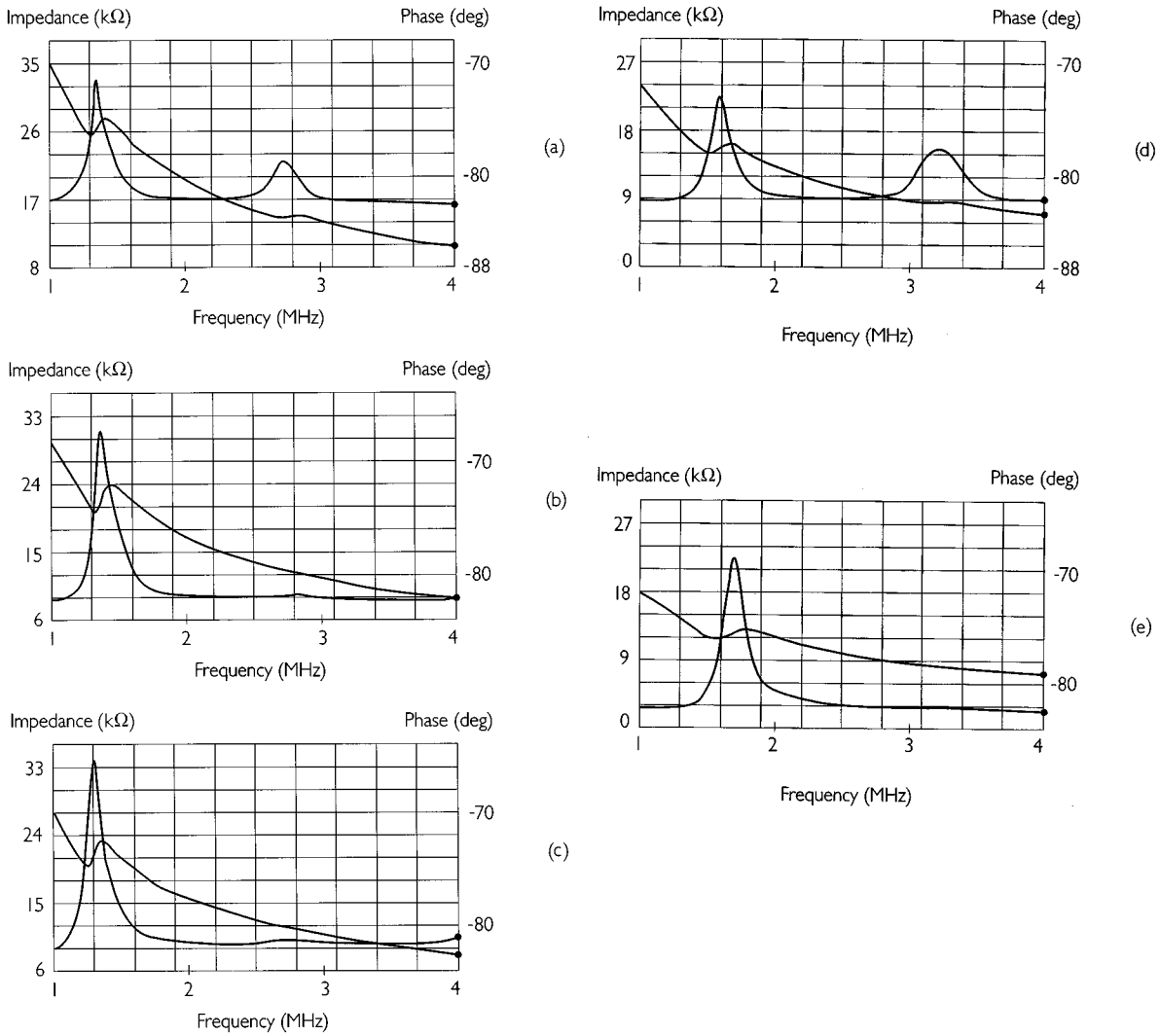

FIG. 3. Impedance and phase vs frequency plot. (a) Sample (i), annealed and poled at 105 °C for 2 h. (b) Sample (ii), annealed and poled at 105 °C for 4 h. (c) Sample (iii), annealed and poled using a two-step poling method. (d) Sample (iv), hot pressed and poled at 115 °C for 1 h. (e) Sample (v), hot pressed and poled using a two-step poling method.

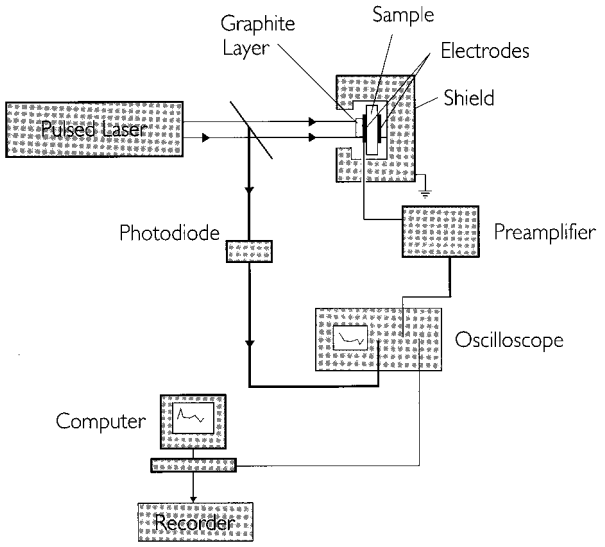

FIG. 4. Experimental set-up used for the laser-induced pressure wave propagation method.

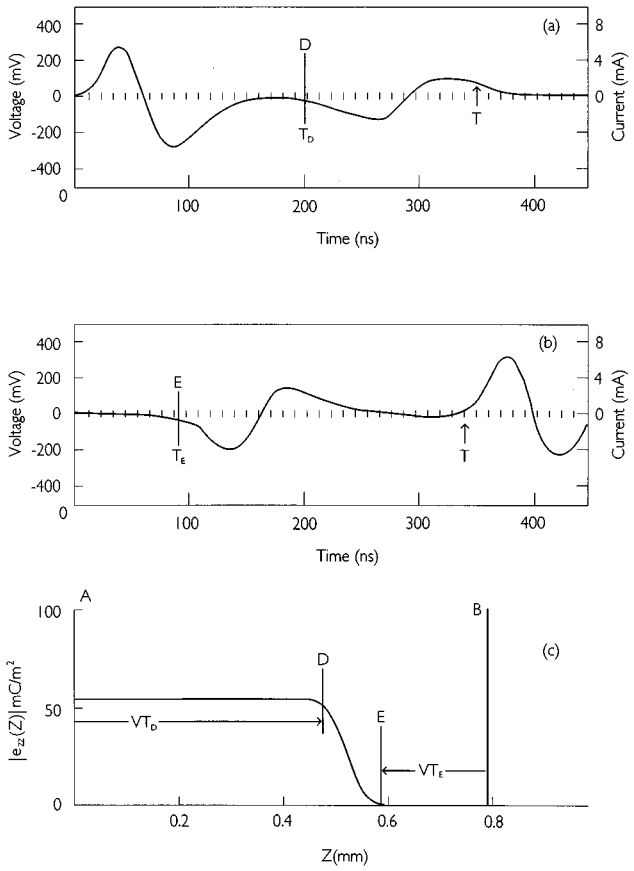

FIG. 5. Short circuit current during the propagation of a pressure pulse in sample (i). The pressure pulse enters the sample at $t=0$, and leaves the sample at $t=T$ as marked by the arrow (T=thickness/velocity), D and E correspond to the locations where sharp changes in polarization were observed, (a) with the pressure pulse entering the sample from the anode (side A), (b) with the pressure pulse entering the sample from the cathode (side B), and (c) schematic $|e_{zz}|$ distribution within the copolymer film (i) from side A to side B.

with a Nd-YAG laser from Spectral Physics, emitting 54 mJ in 30 ns. at 1.06 μm wavelength, with a beam diameter of 8 mm. The laser beam impinges on the surface of a copolymer sample enclosed in an electrically shielded sample holder, and the laser energy is absorbed by a sprayed-on black paint on the sample surface. Due to ablation and localized heating, a pressure pulse is generated which propagates along the z axis (sample thickness direction) with the velocity of sound v. The additional polarization $dP(z)$ arises from two effects: the increase in concentration of the dipoles associated with the permanent polarization, and the generation of new dipoles due to intrinsic piezoelectric effect. The polarization change $dP(z)$ is related to the z component of the strain s_z by

$$dP(z)=e_{zz}(z)s_z, \tag{1}$$

where e_{zz} is the piezoelectric stress coefficient. Consequently, charges are induced in the compressed region, producing an image charge $\Delta Q(z)$ on the electrodes. In short-circuit conditions, the variation of the image charge results in a current $I(t)$ where the time t is related to the position of the wave front by $t=z/v$.

For short pressure pulses, the current measured during the penetration of the pulse into the sample or its exit is directly proportional to the piezoelectric coefficient $e_{zz}(z)$ at the interface[19]

$$I(t)=-a\chi\Delta p(v/d_0)e_{zz}(z), \tag{2}$$

where a is the laser beam area on the target, χ is the compressibility of the material, d_0 is the sample thickness, and Δp is the amplitude of the pressure wave. During its propagation in the sample, $I(t)$ is proportional to $de_{zz}(z)/dz$[18–20]

$$I(t)=-a\chi\Delta p(v^2\tau/d_0)\left[\frac{\partial e_{zz}(z)}{\partial z}\right], \tag{3}$$

where τ is the pressure pulse duration. Figures 5(a), 6(a), 7(a), 8(a), and 9(a), show the signals obtained in short-circuit conditions for a pressure pulse propagating from side A to side B, where side A of the copolymer sample is the one connected to positive poling voltage (the anode) and side B is connected to ground (the cathode). Figures 5(b), 6(b), 7(b), 8(b), and 9(b) show the corresponding signal for the reverse direction of propagation (from side B to side A). It is noted that the bipolar signal generated here results from the relatively thick spray-on black target. If a thin black target (e.g., a thin layer painted using a black marker pen) is used, a single positive or negative peak will result. The bipolar signal observed at the first electrode polymer interface is probably due to an overshoot in the generation of the pressure wave resulting from the impact of the laser pulse on the target. This effect depends on the nature and on the thickness of the target. The presence of a constraining medium on the target surface reduces this overshoot. For thick targets it depends also on the acoustic mismatch between the target and the sample. The effects of using different targets on the shape of the PWP wave form have been discussed elsewhere.[32–34] The velocity of sound v in the copolymer samples, measured using the immersion method,[35] and the sample thickness d_0 are tabulated in Table I. Samples (iv)

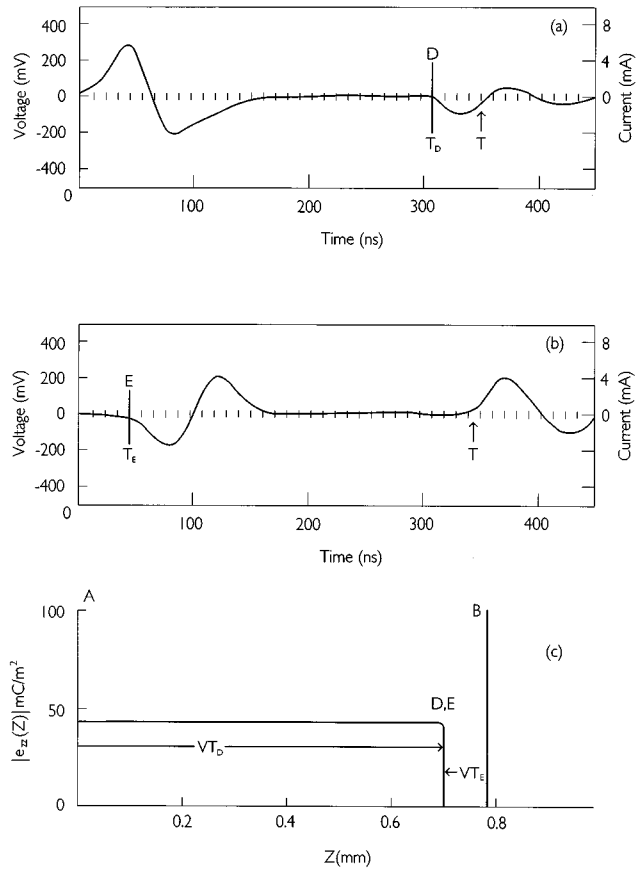

FIG. 6. Short circuit current during the propagation of a pressure pulse in sample (ii). The pressure pulse enters the sample at $t=0$, and leaves the sample at $t=T$ as marked by the arrow (T=thickness/velocity), D and E correspond to the locations where sharp changes in polarization were observed, (a) with the pressure pulse entering the sample from the anode (side A). (b) with the pressure pulse entering the sample from the cathode (side B), and (c) schematic $|e_{zz}|$ distribution within the copolymer films (ii) from side A to side B.

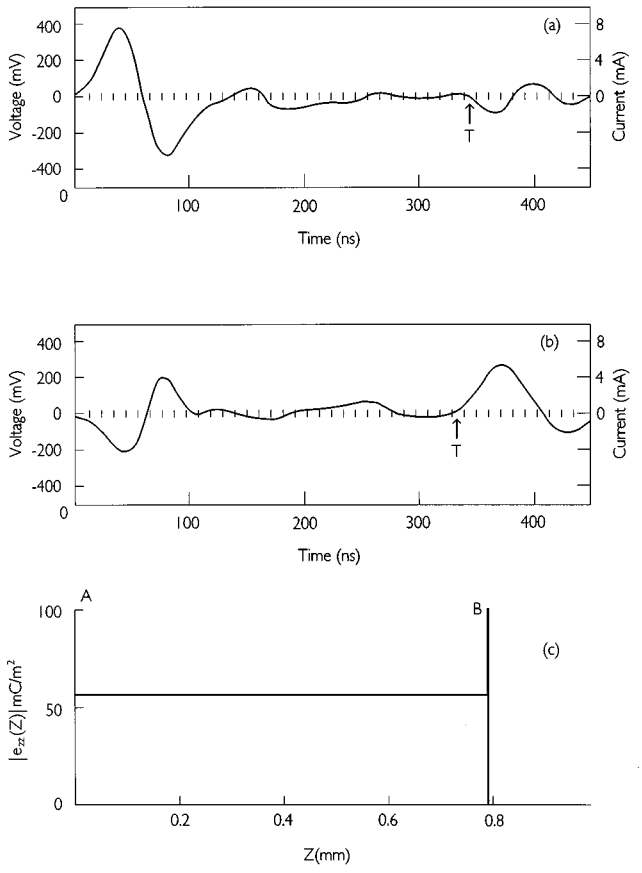

FIG. 7. Short circuit current during the propagation of a pressure pulse in sample (iii). The pressure pulse enters the sample at $t=0$, and leaves the sample at $t=T$ as marked by the arrow (T=thickness/velocity), (a) with the pressure pulse entering the sample from the anode (side A), (b) with the pressure pulse entering the sample from the cathode (side B), and (c) schematic $|e_{zz}|$ distribution within the copolymer films (iii) from side A to side B.

and (v) are thinner because of the melt and hot-pressed heat treatment. Figs. 5(c), 6(c), 7(c), 8(c), and 9(c) show the schematic variation of $|e_{zz}|$ inside the copolymer samples. The values of $|e_{zz}|$ are estimated using the first positive or negative peak of the PWP signal. The fact that $|e_{zz}|$ is constant near the anode can be deduced from Fig. 5(b) [also from Figs. 6(b) to 9(b)] as the PWP signal is flat before the exit T. Locations D and E are where sharp changes in polarizations are detected as marked in Figs. 5(a) and 5(b), 6(a) and 6(b) etc. A method for estimating $|e_{zz}|$ is described in the next section.[36]

B. Estimation of e_{zz}

A 0.8 mm thick x-cut quartz plate[37] with $e_{11}=0.171$ C/m^2, density $\rho_Q=2700$ kg/m^3 and velocity of sound $v_Q=5676$ m/s was used to measure the mechanical momentum $\Delta p\tau a$ generated by the laser beam. If the lateral sample dimensions do not change during the transit of the compression wave, and assuming that the compressibility χ does not depend on pressure and frequency, one has

$$\chi=-1/(\rho v^2). \tag{4}$$

Hence Eqs. (2) and (4), can be used to describe the situation at the entrance interfaces ($t=0$). The amplitude of the entrance current peak ΔI_{input} can be calculated using

$$\Delta I_{\text{input}}=[a\Delta p/(\rho v d_0)]\Delta e_{zz}(0). \tag{5}$$

By integrating this expression over the time of penetration of the pressure wave in the piezoelectric material, we obtain,

$$\left[\int I(t)dt\right]_{\text{input}} \cong \tau\Delta I_{\text{input}}=[a\Delta p\tau/(\rho v d_0)]\Delta e_{zz}(0). \tag{6}$$

In the case where the sample is an x-cut quartz with $\Delta e_{zz}(0)=e_{11}$ the mechanical momentum M can be expressed as

$$M=\Delta p\tau a=\left[\int I(t)dt\right]_Q [\rho_Q v_Q d_Q]/[e_{11}], \tag{7}$$

where $[\int I(t)dt]_Q$ is the area under the first peak of the PWP response and d_Q is the thickness of the x-cut quartz. Assume that the laser-pulse amplitude and the beam area a are approximately constant from pulse to pulse and neglecting the impedance mismatch between the target and the material, the piezoelectric constant e_{zz} of the copolymer can be estimated as

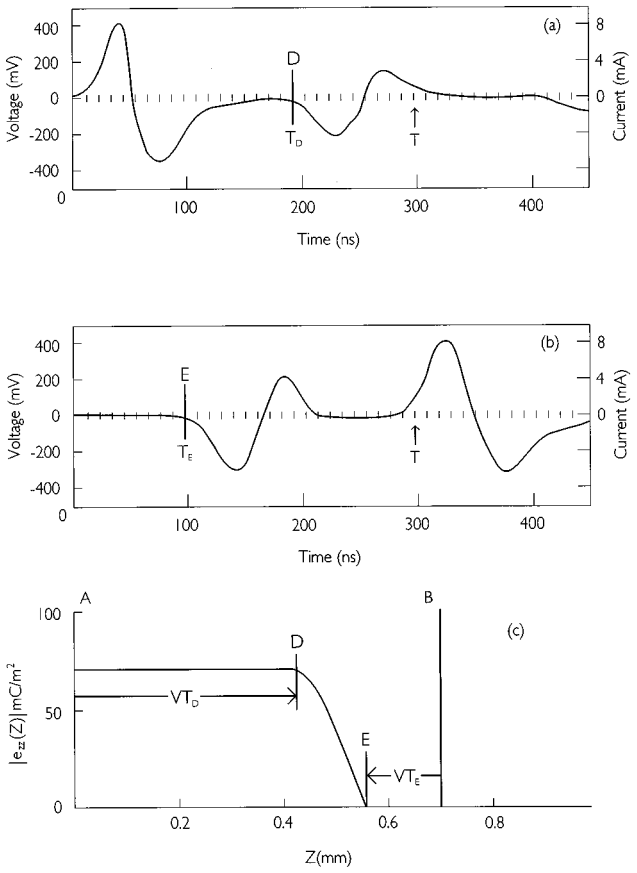

FIG. 8. Short circuit current during the propagation of a pressure pulse in sample (iv). The pressure pulse enters the sample at $t=0$, and leaves the sample at $t=T$ as marked by the arrow (T=thickness/velocity), D and E correspond to the locations where sharp changes in polarization were observed, (a) with the pressure pulse entering the sample from the anode (side A), (b) with the pressure pulse entering the sample from the cathode (side B), and (c) schematic $|e_{zz}|$ distribution within the copolymer film (iv) from side A to side B.

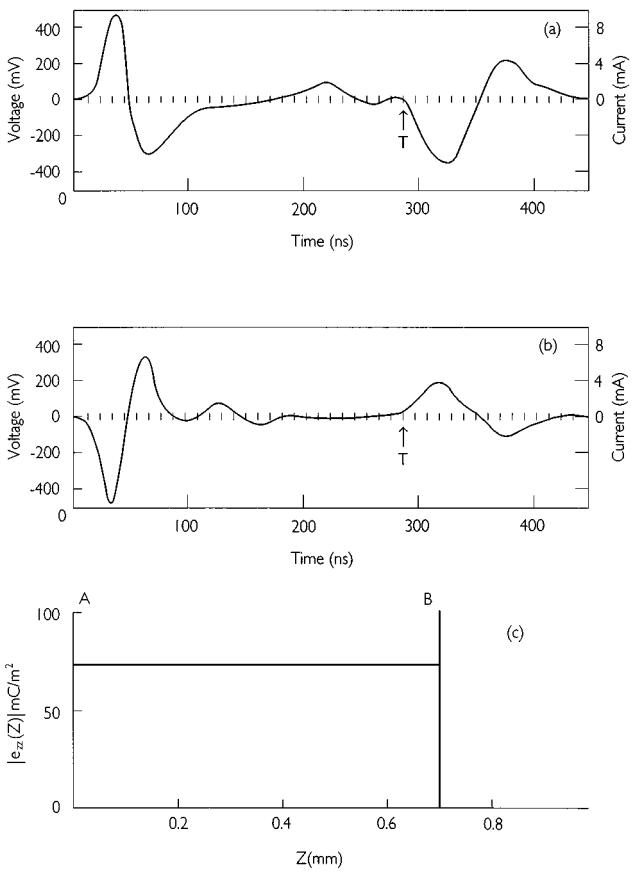

FIG. 9. Short circuit current during the propagation of a pressure pulse in sample (v). The pressure pulse enters the sample at $t=0$, and leaves the sample at $t=T$ as marked by the arrow (T=thickness/velocity), (a) with the pressure pulse entering the sample from the anode (side A), (b) with the pressure pulse entering the sample from the cathode (side B), and (c) schematic $|e_{zz}|$ distribution within the copolymer film (v) from side A to side B.

$$e_{zz}=\left[\int I(t)dt\right]_c \rho v d_0/[M] \tag{8}$$

where $[\int I(t)dt]_c$ is the area under the first peak of the response as the pressure pulse is entering the copolymer. The $|e_{zz}|$ estimated for the five copolymer samples are shown schematically in Figs. 5(c), 6(c), 7(c), 8(c), and 9(c).

IV. RELATION BETWEEN RESONANCE CHARACTERISTICS AND UNIFORMITY OF POLARIZATION IN THE COPOLYMER

In a previous study[24] of the polarization of P(VDF-TrFE) copolymer films (150 μm thick) at 100 °C, it was found that the polarization in this material was very inhomogeneous. The inhomogeneous polarization can be attributed to the presence of a negative space charge which enhances the applied field in the region close to the anode and stabilizes the oriented dipoles. Such a space charge can originate either from the migration of internal charges due to the applied field or from the injection of electrons at the cathode, followed by migration towards the anode.

In the present work, five thick copolymer films were polarized and the polarization distributions and resonance frequencies were then measured. A correlation between the uniformity of the polarization and the resonance characteristics of each sample was made. The polarization distribution was observed to be inhomogeneous and has a noticeable effect on the resonance characteristics of the copolymer film which will affect its use in transducer applications.

In the following we will describe the behavior of the currents measured by the PWP method and will show how a qualitative evaluation of the polarization distribution can be obtained using the theoretical framework given above.

Sample (i). Figures 5(a) and 5(b) show the currents for two directions of propagation of the pressure wave in sample (i): (a) with the pressure wave entering the sample from the anode (side A) and (b) with the pressure wave entering the sample from the cathode (side B). In both cases time $t=0$ represents the time of penetration of the wave into the sample. In the case of curve (a) there is an immediate current response which indicates that the penetrated region exhibits piezoelectric activity. In the case of curve (b) the penetrated region has no piezoelectricity. There are current responses at the interface between the poled and unpoled regions and upon exit of the wave. Curve (c) shows the piezoelectric

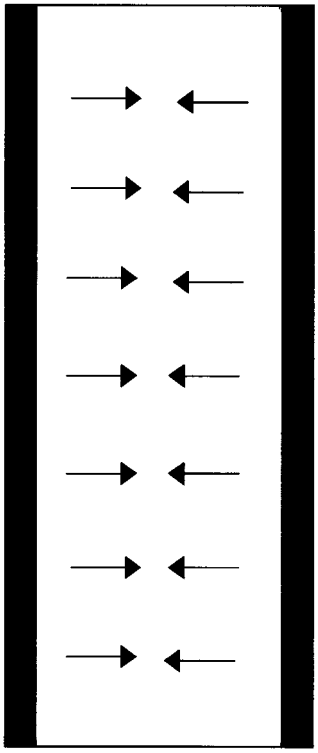

FIG. 10. Thick copolymer film with a bimorph polarization profile.

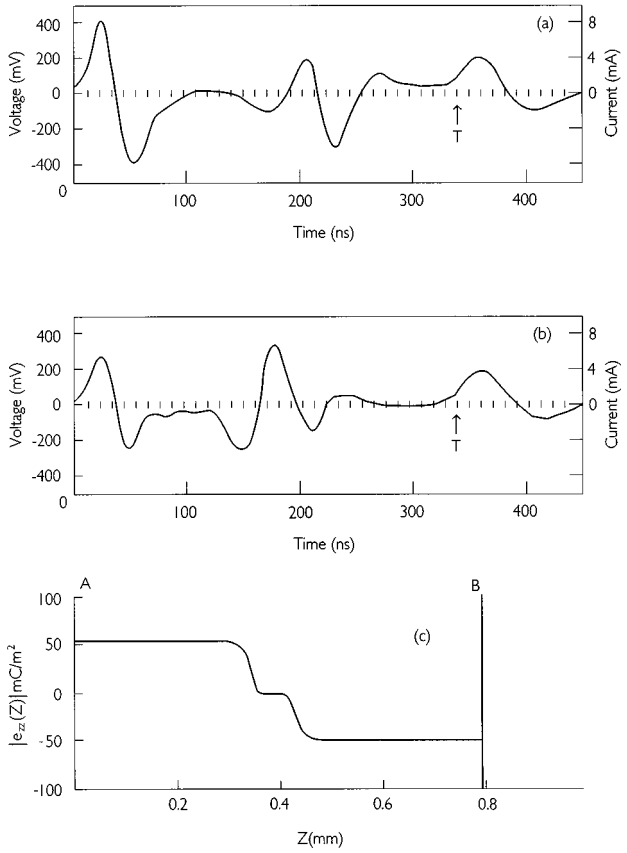

FIG. 11. (a) Short circuit current during the propagation of a pressure pulse in the ''bimorph'' sample with the pressure pulse entering the sample from side A (the side connected to high voltage in the first poling step and connected to ground during the second poling step). (b) Short circuit current during the propagation of a pressure pulse in the ''bimorph'' sample with the pressure pulse entering the sample from side B (the side connected to ground in the first poling and connected to high voltage in the second poling step). (c) Schematic $|e_{zz}|$ distribution within the bimorph from side A to side B.

activity as a function of position in the sample as deduced from curves (a) and (b). Thus after poling for 2 h, only the first half of the sample near the anode has been polarized. The fundamental (1.3 MHz) and the second harmonic (2.6 MHz) frequencies can be excited in this film simultaneously [Fig. 3(a)] and the film has a dual thickness mode. The lower resonance frequency corresponds to the mechanical resonance over the whole thickness of the sample whereas the higher frequency corresponds to the resonance mode of only the polarized region.

Sample (ii). Figure 6 shows the results obtained for sample (ii). A similar analysis can be made. After poling for 4 h. about 80% of the thickness starting from the anode is poled. The second harmonic is barely observable [Fig. 3(b)].

Sample (iii). The results are shown in Fig. 7. This sample was poled using the two step poling method described in Sec. II B. The sample was uniformly poled throughout the whole thickness and the second harmonic is again barely observable [Fig. 3(c)].

Sample (iv). This sample was hot pressed. Figure 8 shows that after poling for 1 h at higher temperature, about half of the thickness has been poled and the fundamental as well as the second harmonic are observed [Fig. 3(d)].

Sample (v). The hot pressed sample was poled using the two step poling procedure. As seen from Fig. 9, the sample has uniform polarization. The second harmonic is not observed [Fig. 3(e)]. This sample has the highest $|e_{zz}|$ [see Figs. 5(c)–9(c)] and the highest k_t (see Table I).

The fact that thick copolymer films can be partially polarized leads to a method for producing bimorphs which is described in the next section.

V. PRODUCTION OF A BIMORPH USING A TWO STEP THERMAL POLING METHOD

The possibility of producing a bimorph structure for thin ($\sim$25 μm) piezopolymers using an electron beam[23] or a thermal method[38] has been reported before. A similar bimorph profile shown schematically in Fig. 10 can be produced in thick copolymer films using a two step thermal poling method.[8,11] If a sample is polarized using a two-step poling process but with the poling field connected in a reversed polarity in the second stage, i.e., side A is connected to ground and side B is connected to high voltage and poled for an equal amount of time (about 1 h for each step) and at the same temperature as in stage 1, a bimorph can be produced. The dipoles inside the copolymer film are polarized in opposite directions in the two halves of the sample and the effective thickness of the film is reduced to half. Figure 11 shows the current in this sample measured by the PWP method. As in the previous paragraph, curve (a) and (b) correspond to the case when the pressure wave penetrates the sample on the anode side (A) and cathode side (B), respectively.

To interpret these data, let us consider the case where there are two regions in a sample (Fig. 12): suppose region I

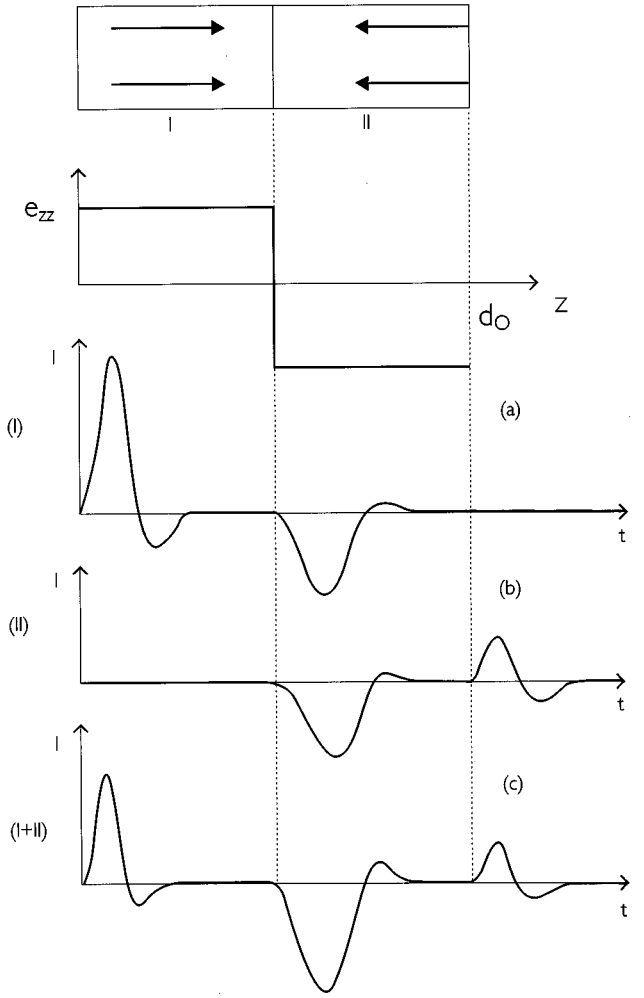

FIG. 12. Schematic drawings to explain the current measured for a perfect bimorph. (a) Current measured for a sample with polarization in the first half of the sample. (b) Current measured for a sample with polarization in the second half of the sample, the polarization has a direction opposite to that in (a). (c) Current measured for a perfect bimorph.

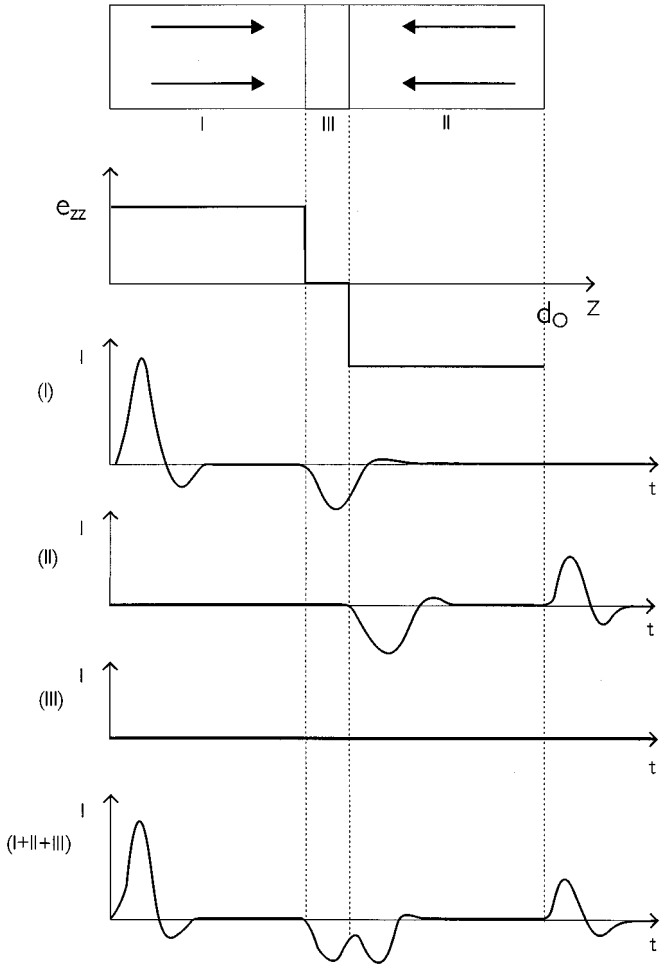

FIG. 13. Schematic drawings showing the current measured for a sample with two regions of opposite polarization and a region with a low polarization in between. The shape of the current oscillation in the middle region will vary with the amount of polarization in the middle region and also with the extent of the middle region.

has a constant polarization whereas region II has zero polarization. The current arising from the pressure wave is shown schematically in Fig. 12(a). We now consider a second sample in which region I has no polarization while region II has a polarization in opposite direction to that of the former one. The current is shown in Fig. 12(b). The current at the interface between the poled and unpoled regions can be predicted as there is perfect impedance matching since the materials in both regions are almost identical. The superposition of the two situations just described leads to the current shown in Fig. 12(c) which corresponds to the case of a perfect bimorph. A comparison between the curve in Figs. 11(a), 11(b), and 12(c) shows that our ''bimorph'' sample has a third region III with a low polarization extending over a short distance between region I and II. This explains the more complicated signals observed in the ''bimorph'' sample [Figs. 11(a) and 11(b)].

To check this interpretation we analyze the case with three regions I, II, and III in a sample. This is shown in Fig.

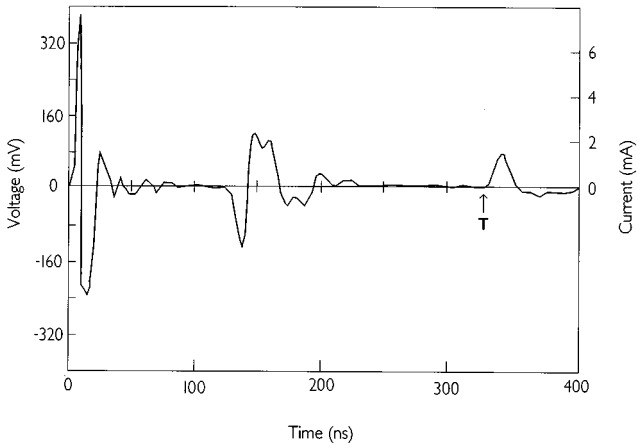

FIG. 14. Current measured (using a 30 ps laser pulse) during the propagation of a pressure pulse in a ''bimorph'' sample with the pressure pulse entering the sample from side A. Improved resolution was obtained compared to Fig. 11(a) and the oscillation showing that there is a region of low polarization in the central region is clearly visible.

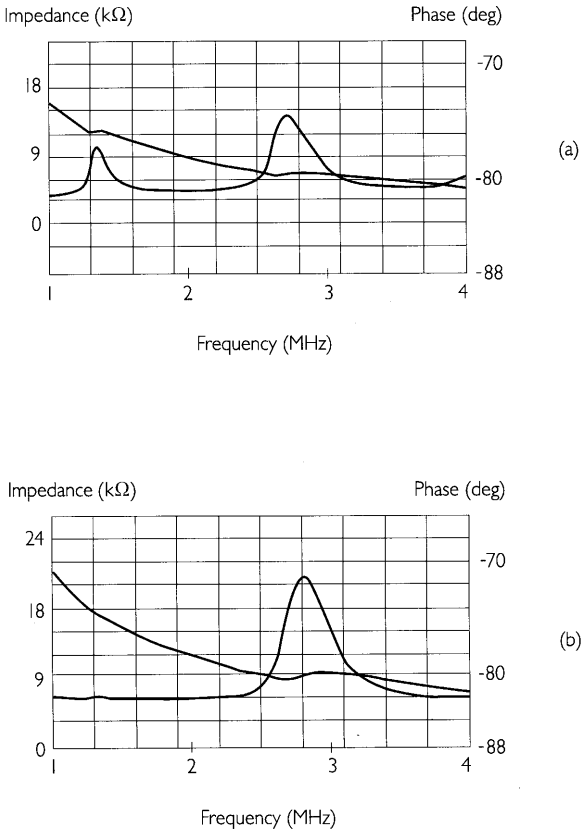

FIG. 15. Impedance and phase vs frequency plot of the copolymer film. (a) After being poled once, showing a dual-frequency resonance. (b) The poling field was reversed in polarity during the second stage poling, resulting in a bimorph structure; the low frequency (1.3 MHz) resonance peak is almost unobservable.

13 which gives the partial currents and the total expected current. In the central region the superposition of the peaks produces an oscillation. In order to check this, we studied the ''bimorph'' sample again using a 30 ps laser pulse which gives an increased resolution. As shown in Fig. 14, the oscillation is indeed observed. The shape of the oscillation is different from that shown in Fig. 13 because the polarization may not be zero in the middle region. Moreover the extent of the low polarization region may be larger that shown in Fig. 13. A comparison of the currents in Figs. 11(a) and 11(b) shows that $|e_{zz}|$ is slightly larger on side A of the sample. The study of resonance peaks for this sample also confirms the above interpretation. As shown in Fig. 15(a), two resonance peaks were observed after the first poling. After poling in the reversed direction, the resonance frequency at 1.3 MHz is almost unobservable and the film has a strong resonance at 2.6 MHz [Fig. 15(b)].

VI. CONCLUSION AND DISCUSSION

Thick films of P(VDF-TrFE) (80/20) copolymer with different heat treatments were poled at high temperature. To obtain high electromechanical coupling constants it is recommended that the film is melted and hot-pressed and then poled by a two-step poling procedure. XRD studies showed that annealing has very little effect on the peaks associated with the polar β phase. However, hot pressing above melting temperature results in a significant change in the magnitude of the diffraction peaks. There is little change in the angle of diffraction (2θ) of the peaks after either heat treatment.

Similar to previous reports on thin films, the polarization in thick P(VDF-TrFE) copolymer films can be very inhomogeneous and this nonuniform polarization affects the resonance characteristics of the films. Using a two-step poling technique but with the poling field reversed in the second step, we can produce a film with a bimorph structure. The bimorph has a single resonance at 2.6 MHz.

In conclusion, a two-step method was used to pole thick copolymer films at high temperature. Further investigations will be necessary to elucidate the mechanisms involved in the two-step poling process. The poled copolymer films with high k_t are useful for fabricating 1–3 composites and for transducer applications. The PWP method is a useful means to map the polarization distribution in a thick copolymer film and the resulting $|e_{zz}|$ value gives an indication of the degree of polarization of the film.

ACKNOWLEDGMENTS

The authors from the Hong Kong Polytechnic University would like to acknowledge the financial support from the Hong Kong Research Grant Council.

[1] M. Latour and R. L. Moreira, IEEE Trans. Electr. Insul. **21**, 525 (1986).
[2] H. Taunaumang, I. L. Guy, and H. L. W. Chan, J. Appl. Phys. **76**, 484 (1994).
[3] C. J. Dias and D. K. Das-Gupta, in *Ferroelectric Polymers and Ceramic-Polymer Composites*, edited by D. K. Das-Gupta (Trans Tech, Switzerland, 1994), p. 217.
[4] K. W. Kwok, H. L. W. Chan, and C. L. Choy, in *Proceedings of the Ninth IEEE Intl. Symp. on Application of Ferroelectrics (ISAF'94)* (IEEE, New York, 1994), p. 194.
[5] H. L. W. Chan, Y. Chen, and C. L. Choy, in *Proceedings of the Ninth IEEE Intl. Symp. on Application of Ferroelectrics (ISAF '94)* (IEEE, New York, 1994), p. 198.
[6] G. T. Davis, M. G. Broadhurst, A. J. Lovinger, and T. Furukawa, Ferroelectrics **57**, 73 (1984).
[7] A. S. DeReggi and M. G. Broadhurst, Ferroelectrics **73**, 351 (1987).
[8] F. I. Mopsik and A. S. DeReggi, Appl. Phys. Lett. **44**, 65 (1984).
[9] S. Ikeda, T. Fukada, and Y. Wada, J. Appl. Phys. **64**, 2026 (1988).
[10] G. M. Sessler, D. K. Das-Gupta, A. S. DeReggi, W. Eisenmenger, T. Furukawa, J. A. Giacometti, and R. Gerhard-Multhaupt, IEEE Trans. Electr. Insul. **27**, 872 (1992).
[11] M. Womes, E. Bihler, and W. Eisenmenger, IEEE Trans. Electr. Insul. **24**, 461 (1989).
[12] G. M. Sessler, in *Ferroelectric Polymers and Ceramic-Polymer Composites*, edited by D. K. Das-Gupta (Trans Tech, Switzerland, 1994), p. 249.
[13] R. E. Collins, J. Appl. Phys. **47**, 4804 (1976).
[14] A. S. DeReggi, C. M. Guttman, F. I. Mopsik, G. T. Davis, and M. G. Broadhurst, Phys. Rev. Lett. **40**, 413 (1978).
[15] S. B. Lang and D. K. Das-Gupta, Ferroelectrics **39**, 1249 (1981).
[16] B. Ploss, R. Emmerich, and S. Bauer, J. Appl. Phys. **72**, 5363 (1992).
[17] A. Cherifi, M. Abou Dakka, and A. Toureille, IEEE Trans. Electr. Insul. **27**, 1152 (1992).
[18] C. Alquié, G. Dreyfus, and J. Lewiner, Phys. Rev. Lett. **47**, 1483 (1981).
[19] C. Alquié and J. Lewiner, Rev. Phys. Appl. **20**, 395 (1985).
[20] G. M. Sessler, J. E. West, R. Gerhard-Multhaupt, and H. von Seggern, IEEE Trans. Nucl. Sci. **NS-29**, 1644 (1983).
[21] W. Eisenmenger and M. Haardt, Solid State Commun. **41**, 917 (1982).
[22] T. Takada, T. Maeno, and H. Kushibe, in *Proc. 5th Intl. Symp. Electrets*, edited by G. M. Sessler and R. Gerhard-Multhaupt (IEEE, New York, 1985), p. 450.

[23] G. M. Sessler and A. Berraissoul, Ferroelectrics **76**, 489 (1987).
[24] C. Laburthe Tolra, C. Alquié, and J. Lewiner, IEEE Trans. Electr. Insul. **EI-28**, 344 (1993).
[25] E. Bihler, K. Holdik, and W. Eisenmenger, IEEE Trans. Electr. Insul. **EI-24**, 541 (1989).
[26] K. Koga and H. Ohigashi, J. Appl. Phys. **59**, 2142 (1986).
[27] P. E. Bloomfield and S. Preis, IEEE Trans. Electr. Insul. **EI-21**, 533 (1986).
[28] H. Ohigashi and K. Koga, Jpn. J. Appl. Phys. **21**, L455 (1982).
[29] M. Latour, in *Ferroelectric Polymers and Ceramic-Polymer Composites*, edited by D. K. DasGupta (Trans Tech, Switzerland, 1994), p. 31.
[30] T. Furukawa, M. Date, M. Ohuchi, and A. Chiba, J. Appl. Phys. **56**, 1482 (1984).
[31] S. Sherrit, H. D. Wiederick, and B. K. Mukherjee, Ferroelectrics **134**, 111 (1992).
[32] C. Alquié, J. Lewiner, and G. Dreyfus, J. Phys. (Paris) Lett. **44**, L-171 (1983).
[33] C. B. Scruby and L. E. Drain, *Laser Ultrasonics: Techniques and Applications* (Hilger, Bristol, 1990), p. 290.
[34] D. A. Hutchins, Can. J. Phys. **64**, 1247 (1986).
[35] B. Hartmann, Method of Experimental Physics 16C (Academic, New York, 1980), p. 59.
[36] R. Gerhard-Multhaupt, G. M. Sessler, and J. E. West, J. Appl. Phys. **55**, 2769 (1984).
[37] J. F. Rosenbaum, *Bulk Acoustic Wave Theory and Devices* (Artech House, Boston, 1988), p. 456.
[38] M. A. Marcus, J. Appl. Phys. **52**, 6273 (1981).